World Academy of Science, Engineering and Technology
International Journal of Structural and Construction Engineering
Vol:15, No:1, 2021

# Lateral-Torsional Buckling of Steel Girder Systems Braced by Solid Web Crossbeams

Ruoyang Tang, Jianguo Nie



***Abstract*—**Lateral-torsional bracing members are critical to the stability of girder systems during the construction phase of steel-concrete composite bridges, and the interaction effect of multiple girders plays an essential role in the determination of buckling load. In this paper, an investigation is conducted on the lateral-torsional buckling behavior of the steel girder system which is composed of three or four I-shaped girders and braced by solid web crossbeams. The buckling load for such girder system is comprehensively analyzed and an analytical solution is developed for uniform pressure loading conditions. Furthermore, post-buckling analysis including initial geometric imperfections is performed and parametric studies in terms of bracing density, stiffness ratio as well as the number and spacing of girders are presented in order to find the optimal bracing plans for an arbitrary girder layout. The theoretical solution of critical load on account of local buckling mode shows good agreement with the numerical results in eigenvalue analysis. In addition, parametric analysis results show that both bracing density and stiffness ratio have a significant impact on the initial stiffness, global stability and failure mode of such girder system. Taking into consideration the effect of initial geometric imperfections, an increase in bracing density between adjacent girders can effectively improve the bearing capacity of the structure, and higher beam-girder stiffness ratio can result in a more ductile failure mode.

***Keywords*—**Bracing member, construction stage, lateral-torsional buckling, steel girder system.

## I. Introduction

STEEL girder system is an intermediate multi-girder structure which typically exists in the construction stage of steel-concrete bridges. The stability of such system largely depends on the layout of cross bracings between the adjacent main girders [1], without which the steel girders would individually bearing the load from the concrete deck, monolithic casting layer and pavement before the adhesive strength come into effect. In order to avoid buckling failure of the whole system and make the most of the post-buckling strength of the temporary members, the cross bracings should be carefully designed. Generally, cross bracings can be divided into two types: cross frames and solid web crossbeams [2]. Solid web crossbeams, temporary members in most cases, are more practically applied in small span bridges since fewer beam-girder joints are needed during erection.

Chinese and Japanese Specifications have specified the maximal longitudinal interval of cross bracings for steel bridges [3], [4]. The inelastic buckling criterion has been enumerated in Korean specification [5], which provides a benchmark to evaluate the stability for braced girder systems. Furthermore, bracing stiffness has been comprehensively considered in American standards [6]-[8], where the design value of linear bend stiffness and relative bracing height are recommended. There has been theoretical investigation on the critical load solution of twin girder systems braced by solid web cross beams developed for a pure moment condition [9]. Also, experimental study on the relative bracing height has been conducted and numerically verified [10].

Most of the regulations and studies, [9], [10], have considered the twin girder system in pure bending case, and empirically adjust for the lateral load case. Moreover, fewer theoretical researches have focused on the braced system with more than two girders. In this paper, the theoretical model for the buckling load of multi-girder system have been put forward and verified by eigenvalue analysis in ABAQUS. Parametric studies have been conducted in order to find the optimal layout for crossbeams and provide a feasible scheme for practical use.

## II. Theoretical Model for Elastic Buckling Behavior

### A. Derivation of Equilibrium Differential Equations

In this paper, the grillage mesh method is adopted to analyze the buckling behavior of girder systems composed of three or four main girders. The equilibrium differential equations for Lateral-torsional buckling are derived under the following hypothesis:

1) Two (three) cross beams are supposed to support through the cross section of the triple (quadruple) girder system at a certain longitudinal position. The rigid-body rotation angle of cross beams within the deck plane is assumed to be global (denoted as $\xi$). Fig. 1 shows the layout of initial and deformed cross beam configuration in the triple (quadruple) girder system.

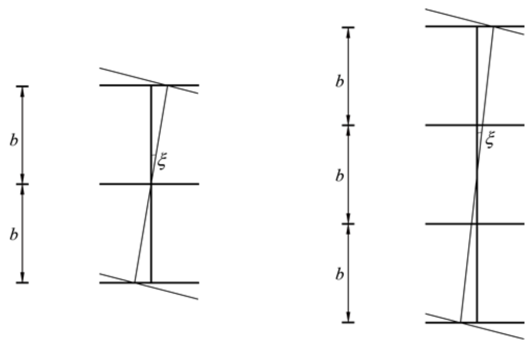


Fig. 1 Initial and Deformed Cross Beam Configuration

Ruoyang Tang is with the Department of Civil Engineering, Tsinghua University, Beijing, China (phone: 86-17888830601; e-mail: try18@mails.tsinghua.edu.cn).

Jianguo Nie is with the Department of Civil Engineering, Tsinghua University, Beijing, China (e-mail: niejg@tsinghua.edu.cn).

2) We denote the space between two adjacent girders is $b$, bending stiffness of the main girder is $EI_{ym}$ with respect to the weak axis and $EI_{xm}$ with respect to the strong axis, bending stiffness of the cross beam is $EI_{yc}$ with respect to the weak axis. Since a single cross beam is shared between two adjacent grillage meshes, only half of the line stiffness is considered in the analysis.
3) The shape of the cross section remains unchanged, which means that the rotation and displacement of the whole section can be properly modeled by the center displacement of the web.
4) The cross beams are uniformly distributed in the major span. The react moment and shear force at the end are assumed to be transformed into uniform moment and uniform axial force exerted on the main girder if multiple cross beams are set up.
5) Although in service stage, joint rigidity between cross beams and main girders is not necessarily maintained due to local distortion under cyclic loading, the rigid joint hypothesis is still adopted in view of a relatively short-term construction stage.

According to the relationship between the displacement and rigid-body rotation of the cross beam in a single grillage mesh, the equilibrium differential equation can be formulated by the introduction of moment equilibrium as demonstrated in (1):

$$EI_{yt}u^{(4)} - EI_{ym}A_t u^{(6)} - \mu\left[\left(M_x\varphi\right)'' - A_t\left(M_x\varphi\right)^{(4)}\right] = 0 \quad (1)$$

In the torsional analysis of the girder system, three components of resistant torque are considered, namely the pure torsion and local warping of each girder section, and global warping of the whole system, as demonstrated in Fig. 2.

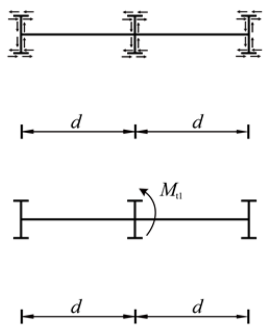


(a) Pure Torsion

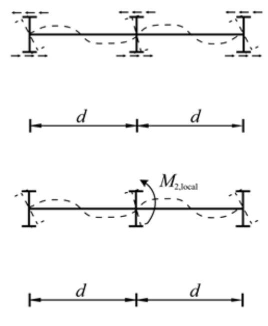


(b) Local Warping of Girder Flanges

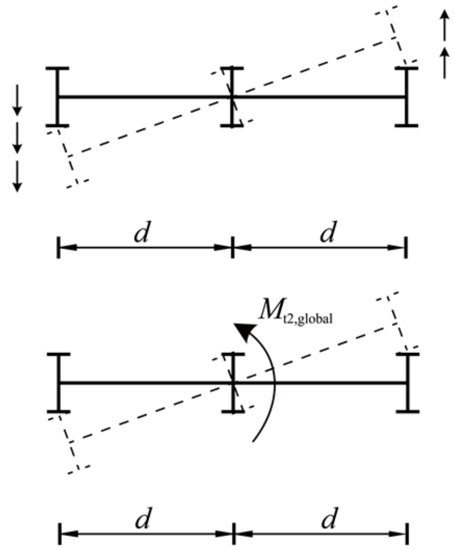


(c) Global Warping of Boundary Girders

Fig. 2 Resistant Torque Component of Girder System

Equilibrium differential equation with respect to torsion can be expressed as shown in (2):

$$M_x u'' + \mu\left(GJ_m\varphi'' - EC_{wt}A_t\varphi^{(4)}\right) = 0 \quad (2)$$

Structural parameters in (1) and (2) are enumerated (see Table III in Appendix), where $k_u$, $k_\varphi$ and $k_v$ respectively stand for the hyper-parameter that is related to girder displacement ratio, girder rotation ratio and local buckling.

*B. Analytical Solution and Numerical Verification*

By applying Galerkin Method, the elastic buckling load could be analyzed for triple or quadruple girder systems. This method, linear combination of optimized shape functions which satisfy displacement and force boundary conditions have been chosen to interpolate the solution. The elastic buckling load can be therefore written as (3):

$$P_{cr} = \frac{2E}{l^3}\sqrt{\frac{I_1 I_4}{I_2 I_3}} \quad (3)$$

$I_1$, $I_2$, $I_3$ and $I_4$ are integration parameters with respect to the optimized shape functions. The relationship between these parameters and structural parameters can be established (see Table IV in Appendix).

In Table I, the parameter reflects the effect that caused by the displacement difference of boundary girders and middle girders, and the parameter $\mu_2$ reflects the effect that comes from the rotational difference. Under the circumstance of local buckling, the stiffness of the global system has little contribution to the buckling load, thus $\mu_1 = \mu_2 = 0$ while in case of global buckling, the effect of global stiffness cannot be ignored, which should be reflected in the value of these two hyper parameters as shown in Table I.

TABLE I
CANDIDATE VALUE OF STRUCTURAL HYPER-PARAMETERS

| Buckling Type | Triple Girder System | Quadruple Girder System |
|---|---|---|
| Global | 2/3 | 5/4 |
| Local | 0 | 0 |

### *C. Numerical Verification and Modification*

For the purpose of numerical verification, the critical buckling load under multiple loading cases is compared with the result from finite element eigenvalue analysis. Considering the actual construction conditions, 750 structural designation cases have been numerically analyzed with respect to different number of major girders, span, girder height and space between girders. The analysis is based ABAQUS eigenvalue analysis and python interface is used to automatically establish bridge models.

According to the finite element eigenvalue analysis, whether local buckling or global buckling will happen depends on the number of girders, girder-crossbeam height ratio, flange thickness of crossbeam, space between girders and number of crossbeams. Typical buckling modes of girders systems are enumerated as in Fig. 3.

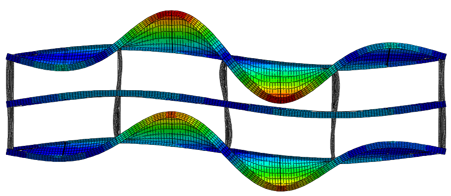

(a) Local Buckling (Triple Girder System)

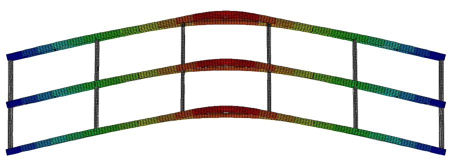

(b) Global Buckling (Triple Girder System)

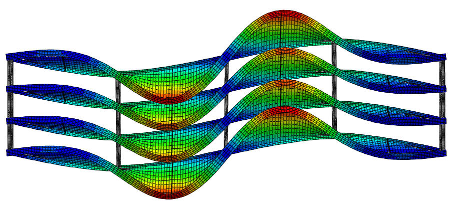

(c) Local Buckling (Quadruple Girder System)

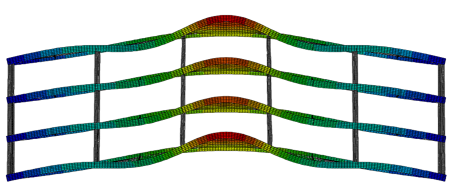

(d) Global Buckling (Quadruple Girder System)

Fig. 3 Typical Buckling Modes of Girder Systems

We set the permitted relative error as 15%, the theoretical and numerical results are compared with respect to local buckling and global buckling (see Table II). It can be seen that if local buckling happens, the theoretical prediction agrees well with the numerical results.

TABLE II
COMPARISON OF THEORETICAL AND NUMERICAL RESULTS

| | Local Buckling | |
|---|---|---|
| | Triple Girder System | Quadruple Girder System |
| Number of Cases within Error Limit | 166 | 149 |
| Total Number of Cases | 169 | 152 |
| Percentage | 98.22% | 98.03% |
| | Global Buckling | |
| | Triple Girder System | Quadruple Girder System |
| Number of Cases within Error Limit | 137 | 123 |
| Total Number of Cases | 206 | 223 |
| Percentage | 66.50% | 55.16% |

In case of global buckling, regression analysis is performed based upon finite element results. The modified theoretical solution is modified as shown in (4). Definition of regression variables and regression results of coefficients can be found in Table V.

$$\bar{p}_{t,cr} = p_{t,cr} \Big/ \prod_{k=1}^{8} \left(\gamma_{k0} + \gamma_{k1} x_k\right) \tag{4}$$

## III. PARAMETRIC STUDY OF STRUCTURAL LAYOUTS USING POST BUCKLING ANALYSIS METHOD

### *A. Effect of Initial Imperfection*

In this subpart, the eigenvalue analysis is performed beforehand to acquire the normalized buckling modes (typically the 3$^{rd}$ and 4$^{th}$ order), which will be exerted on the system as the initial imperfection in the post-buckling analysis. The 1$^{st}$ order buckling mode in the eigenvalue analysis is taken as fundamental. Moreover, two typical kinds of static load patterns (namely the bending in and out) are exerted on the system, and the deformed configurations are treated as initial imperfection types. Analysis results are shown in Fig. 4.

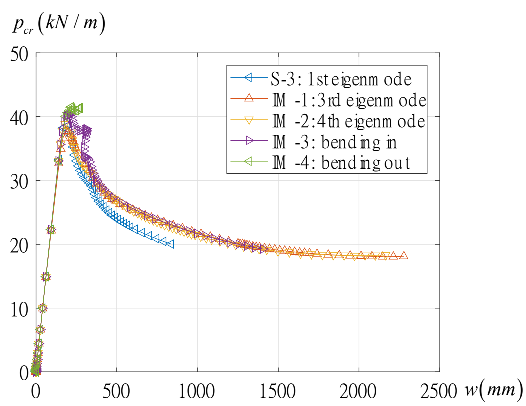


Fig. 4 Load-deflection Curve of Middle Span under Different Initial Imperfection Types

It can be seen that initial imperfection types have little effect on the initial system stiffness and ductility in the failure stage. Comparing with IM-2, IM-3 has larger initial imperfection in one of the boundary girders, and the initial rotation gradually resumes as the load increases, which explains a higher bearing load than IM-2. For similar reason, since both boundary girders initially deformed outward, IM-4 reaches the largest bearing load among the study groups. S-1 is found to be the worst initial imperfection type, which will be adopted in the following researches.

*B. Effect of Girder-crossbeam Height Ratio*

Take triple girder systems with two crossbeams equally distributed between each group of adjacent girders as instance, the girder-crossbeam ratio ranges from 0.25 to 0.75. The loading load-displacement curves are shown in Fig. 5.

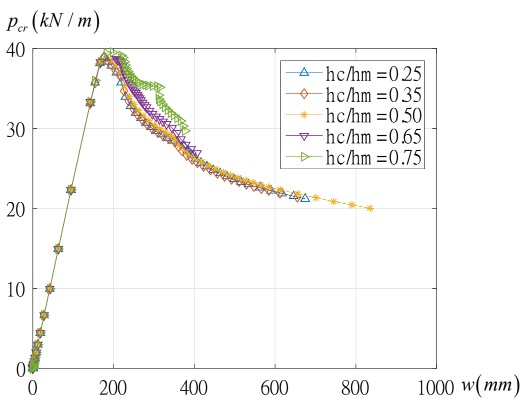


(a) Load-deflection Curve of Middle Span under Different Girder-crossbeam Height Ratios

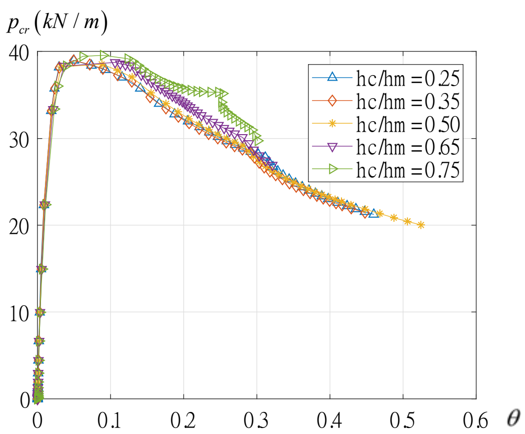


(b) Load-rotation Curve of Middle Span under Different Girder-crossbeam Height Ratios

-Fig. 5 Load-displacement Curve of Middle Span under Different Girder-crossbeam Height Ratios

It can be seen from Fig. 5 (a) that the load has linear relationship with the deflection, which means that the increase of relative height of crossbeam has little effect on the initial system stiffness. Failure ductility can be seen from all the study cases. When the bearing load declines to half of the peak value, the deflection increases by 4 times than the peak point, and the rotation increases by 6 times.

The system stability capacity is far less vulnerable to the girder-crossbeam height ratio. Since crossbeam stiffness contribute trivially to the equivalent section area of the girder system. As can be seen from Fig. 6, the theoretical solution of local buckling is lower than the numerical eigenvalue solution by approximately 7%, while the ultimate bearing capacity in post-buckling analysis only account for 65% to 75% of the eigenvalue solution since material nonlinearity and initial imperfection exists.

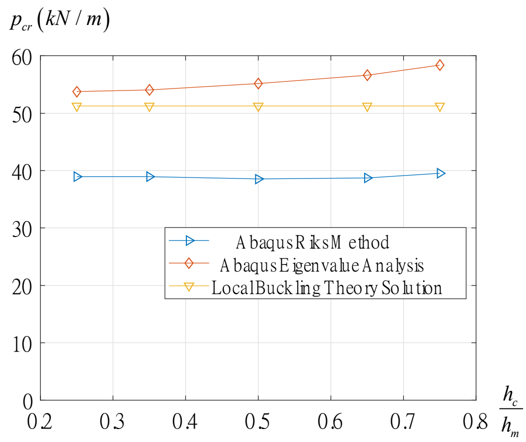


Fig. 6 Critical Load with Respect to Girder-crossbeam Height Ratio

*C. Effect of Crossbeam Density*

We take triple girder systems with girder-crossbeam height ratio equal to 0.65 as example, the number of crossbeams between each group of adjacent girders is selected as 4, 5 or 6. The load-deflection curve can be extracted as shown in Fig. 7.

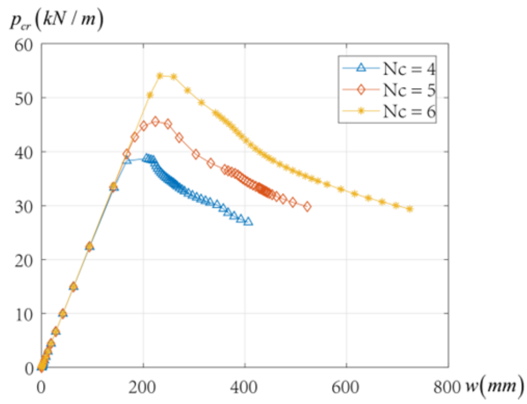


Fig. 7 Load-deflection Curve of Middle Span under Different Crossbeam Density ($h_c/h_m = 0.65$)

It can be seen that the crossbeam density has significant effect on the bearing capacity of the girder system, while has trivial impact on the initial system stiffness. However, as the girder-crossbeam height ratio increases, the crossbeam density effect becomes less significant as shown in Fig. 8.

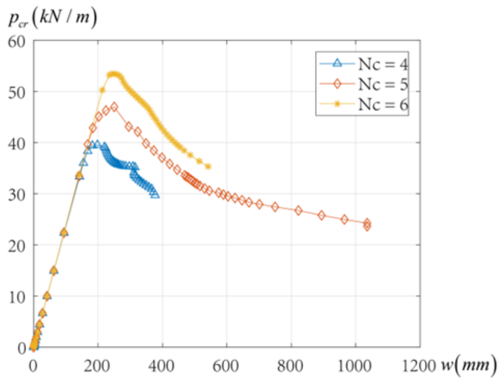


Fig. 8 Load-deflection Curve of Middle Span under Different Crossbeam Density ($h_c/h_m = 0.75$)

## IV. Conclusion

Aiming at triple and quadruple girder systems bearing uniformly distributed line load, this research has put forward a theoretical solution that accounts for the elastic buckling load. On the one hand, the analytical result agrees well with the critical load from numerical eigenvalue analysis under the circumstance of local buckling mode. On the other hand, for global buckling systems, the analytical solution needs to be modified by structural parameters.

Parametric comparative studies have been carried out and it is found out that girder-crossbeam height ratio and crossbeam density are the two major factors that influence the failure mode and stability bearing capacity of girder systems. For further research purposes, the percentage of the reduction of bearing capacity needs to be investigated considering the effect of initial imperfection and material nonlinearity, which will provide supportive theoretical models and engineering formula for crossbeam designation.

## Appendix

Structural parameters for equilibrium differential equations have been listed in Table III.

TABLE III
Structural Parameters of Equilibrium Equations

| Var | Triple Girder System |
|---|---|
| $EI_{yt}$ | $EI_{ym}+\mu_1 EA_m b^2$ |
| $EC_{wt}$ | $EC_{wm}+\mu_2 EI_{xm} b^2$ |
| $A_t$ | $\left(6b^4dI_{ym}^2+6b^3d^2I_{ym}I_{yc}+b^2d^3I_{yc}^2\right)A_m/\left(72bI_{ym}^2I_{yc}+18dI_{ym}I_{yc}^2\right)$ |
| $\mu_1$ | $2/\left(k_u+2\right)$ |
| $\mu_2$ | $2k_v/\left(k_\varphi+2\right)$ |
| $\mu$ | $\left(k_\varphi+2\right)/\left(k_u+2\right)$ |
| **Var** | **Quadruple Grider System** |
| $EI_{yt}$ | $EI_{ym}+\mu_1 EA_m b^2$ |
| $EC_{wt}$ | $EC_{wm}+\mu_2 EI_{xm} b^2$ |
| $A_t$ | $\left(60b^4dI_{ym}^2+70b^3d^2I_{ym}I_{yc}+15b^2d^3I_{yc}^2\right)A_m/\left(216bI_{ym}^2I_{yc}+72dI_{ym}I_{yc}^2\right)$ |
| $\mu_1$ | $5/\left(2k_u+2\right)$ |
| $\mu_2$ | $5k_v/\left(2k_\varphi+2\right)$ |
| $\mu$ | $\left(k_\varphi+1\right)/\left(k_u+1\right)$ |

Integration parameters with respect to structural parameters for the calculation of theoretical buckling loads are provided in Table IV.

TABLE IV
Integration Parameters of Analytical Solution

| Var | Case 1: Global Buckling |
|---|---|
| $I_1$ | $48.70I_{yt}+480.7A_tI_{ym}/l^2$ |
| $I_2$ | $450.06A_t/l^2+1.073$ |
| $I_3$ | $1.073$ |
| $I_4$ | $48.70C_{wt}/l^2+2.467J_m/\left(1+v\right)$ |
| **Var** | **Case 2: Local Buckling ($N_c$=4)** |
| $I_1$ | $4421I_{yt}+4.678\times10^5A_tI_{ym}/l^2$ |
| $I_2$ | $1180A_t/l^2+9.211$ |
| $I_3$ | $9.211$ |
| $I_4$ | $4421C_{wt}/l^2+23.21J_m/\left(1+v\right)$ |
| **Var** | **Case 3: Local Buckling ($N_c$=5)** |
| $I_1$ | $1.347\times10^5I_{yt}+2.32\times10^6A_tI_{ym}/l^2$ |
| $I_2$ | $3165A_t/l^2+16.02$ |
| $I_3$ | $16.02$ |
| $I_4$ | $1.347\times10^5C_{wt}/l^2+41.02J_m/\left(1+v\right)$ |
| **Var** | **Case 4: Local Buckling ($N_c$=6)** |
| $I_1$ | $3.233\times10^5I_{yt}+8.4\times10^6A_tI_{ym}/l^2$ |
| $I_2$ | $7099A_t/l^2+24.76$ |
| $I_3$ | $24.76$ |
| $I_4$ | $3.233\times10^5C_{wt}/l^2+63.92J_m/\left(1+v\right)$ |
| **Var** | **Case 5: Local Buckling ($N_c$=7)** |
| $I_1$ | $6.643\times10^5I_{yt}+2.443\times10^7A_tI_{ym}/l^2$ |
| $I_2$ | $1.401\times10^5A_t/l^2+35.45$ |
| $I_3$ | $35.45$ |
| $I_4$ | $6.643\times10^5C_{wt}/l^2+91.91J_m/\left(1+v\right)$ |
| **Var** | **Case 6: Local Buckling ($N_c$=8)** |
| $I_1$ | $1.224\times10^6I_{yt}+6.066\times10^7A_tI_{ym}/l^2$ |
| $I_2$ | $2.518\times10^5A_t/l^2+48.07$ |
| $I_3$ | $48.07$ |
| $I_4$ | $1.224\times10^6C_{wt}/l^2+125J_m/\left(1+v\right)$ |

For the purpose of theoretical modification, the regression results are enumerated in Table V.

TABLE V
Regression Variable Definition and Results

| Variable | Definition | Coefficient | Result | Coefficient | Result |
|---|---|---|---|---|---|
| $x_1$ | $N_m$ | $\gamma_{10}$ | 0.7148 | $\gamma_{11}$ | 0.08102 |
| $x_2$ | $b/l$ | $\gamma_{20}$ | 0.7230 | $\gamma_{21}$ | 3.099 |
| $x_3$ | $h_c/h_m$ | $\gamma_{30}$ | 1.069 | $\gamma_{31}$ | -0.1318 |
| $x_4$ | $N_c$ | $\gamma_{40}$ | 0.4955 | $\gamma_{41}$ | 0.07193 |
| $x_5$ | $I_{xc}/I_{xm}$ | $\gamma_{50}$ | 1.233 | $\gamma_{51}$ | -1.103 |
| $x_6$ | $I_{yc}/I_{ym}$ | $\gamma_{60}$ | 0.9072 | $\gamma_{61}$ | 1.244 |
| $x_7$ | $J_c/J_m$ | $\gamma_{70}$ | 0.9542 | $\gamma_{71}$ | 0.5603 |
| $x_8$ | $C_{wc}/C_{wm}$ | $\gamma_{80}$ | 1.016 | $\gamma_{81}$ | -0.7094 |

## References

[1] Nie Jian-Guo, *Steel-Concrete Composite Bridges*. Beijing: China

Communication Press, 2011.

[2] J. P. Lebet, M. A. Hurt, Ge Yao-Jun, Su Qing-Tian *Conceptual and Structural Design of Steel and Steel-concrete Composite Bridges.* Beijing: China Communication Press, 2014.

[3] Ministry of Railways of the People's Republic of China, *Code for Design on Steel Structure of Railway Bridge*, TB 10002.2-2005/J 461-2005. China Railway Publishing House, 2005.

[4] Japan Road Association, *Reference for Railway Bridge - Steel Bridge*, Ethylene Chemical CO: 2001.

[5] KRTA, *Standard specifications for roadway bridges*, Seoul, Korea: Korean Road and Transportation Association, 2005.

[6] AISC, *Steel construction manual*, Chicago: American Institute of Steel Construction, 2005.

[7] SSRC, *Guide to stability design criteria for metal structures*, New York: Wiley, 2009.

[8] AASHTO, *Standard specifications for highway bridges*, Washington DC: American Association of State Highway and Transportation Officials, 2002.

[9] Sadao Komatsu, Nobuo Nishimura, Masato Ohno, “Overall Lateral Buckling of Ladder-like Plate Girder Bridges and Its Stiffening Design Method”, Proceedings of the Japan Society of Civil Engineers, 1983, vol. 1983, Issue 329, pp. 69-79.

[10] Mehri H, Crocetti R. “Effects of Geometric Imperfections on the Bracing Performance of Cross Beams during Construction of Composite Bridges”, Bridge Eng, 2017, 22(1).